

# Cubic Stabilized Zirconium Oxide Anodic Films Prepared at Room Temperature

E. O. Bensadon,<sup>†</sup> P. A. P. Nascente,<sup>‡</sup> P. Olivi,<sup>§</sup> L. O. S. Bulhões,<sup>†</sup> and E. C. Pereira<sup>\*,†</sup>

*Laboratório Interdisciplinar de Eletroquímica e Cerâmica, Departamento de Química, and Centro de Caracterização e Desenvolvimento de Materiais, Departamento de Engenharia de Materiais, Universidade Federal de São Carlos, 13565-905, São Carlos, SP, Brazil, and Faculdade de Filosofia, Ciências e Letras, Universidade de São Paulo, Campus de Ribeirão Preto, 14040-901, Ribeirão Preto, SP, Brazil*

Received July 17, 1998. Revised Manuscript Received October 5, 1998

A new methodology was developed to obtain cubic, stabilized zirconium oxide films prepared at room temperature. The zirconium oxide films were prepared electrochemically by anodic oxidation of metallic zirconium at constant current density. The oxide films were analyzed by X-ray diffraction, scanning electron microscopy, and X-ray photoelectron spectroscopy. The oxide films grown in H<sub>3</sub>PO<sub>4</sub> solutions are monoclinic, and the ones prepared in phosphoric acid solution containing Na<sub>2</sub>[Ca(EDTA)] complex are cubic. An explanation for the zirconium oxide stabilization obtained by the electrochemical method is proposed that assumes a destruction and rebuilding of the oxide film during the dielectric breakdown.

## Introduction

Zirconium oxide, known as zirconia, is a material extensively used in industry as refractory and oxygen sensor materials.<sup>1</sup> However, for any of its applications it is necessary to control its crystal structure. At room temperature, pure zirconium oxide occurs in the monoclinic phase changing to the tetragonal phase at 1270 °C. At temperatures close to 2370 °C, the tetragonal zirconium oxide becomes cubic, and it melts at 2680 °C. The tetragonal to cubic phase transformation is reversible. On the other hand, the tetragonal to monoclinic transformation occurs throughout cooling, with thermal hysteresis at 950 °C. During the transformation from tetragonal to monoclinic phase, a mechanic degradation process occurs due to the larger molar volume of the tetragonal phase (3–5%). High temperatures are necessary in ceramic processing; therefore, the tetragonal to monoclinic transformation must be prevented during the material cooling. The preparation of stabilized zirconium oxide films in either tetragonal or cubic phase can be made by different methods, such as the oxide mixture and chemical methods.<sup>2</sup> Another method used is doping the oxide with CaO, MnO, MgO, Nb<sub>2</sub>O<sub>5</sub>, or Y<sub>2</sub>O<sub>3</sub>, which form solid solutions with ZrO<sub>2</sub>. These dopants inhibit the transformation from the tetragonal (or cubic) to the monoclinic phase during cooling.<sup>3,4</sup>

Several papers describe the electrochemical formation of the zirconium oxide films on metallic zirconium substrate at room temperature.<sup>5–10</sup> The zirconium oxide obtained by electrochemical methods crystallizes during the film growth in the monoclinic phase. At very high fields, a dielectric breakdown occurs, resulting in fracture of the oxide film and formation of pores. The film is quickly regenerated, leading to a high local current densities in the pores. Considering the conditions of the breakdown and rebuilding processes during the film growth and the fact that solution anions migrate into the film during the breakdown process and can be incorporated into the oxide film structure, we decided to investigate the effect of the addition of Ca<sup>2+</sup> complex ions to the solution. This process can generate solid solutions in ZrO<sub>2</sub>, allowing the cubic phase stabilization. In this paper we present a new electrochemical method for preparing a stabilized zirconium oxide film, as well as the results of the film characterization by X-ray diffraction (XRD), scanning electron microscopy (SEM), and X-ray photoelectron spectroscopy (XPS).

## Materials and Methods

The oxide films were grown anodically on a zirconium substrate in 0.1 mol L<sup>-1</sup> phosphoric acid aqueous solution at a constant current density. Initially, the oxide films prepared in acid aqueous solution with no dopant ions were studied. Then, the oxide films formed in 0.1 mol L<sup>-1</sup> phosphoric acid

\* Corresponding author. E-mail: decp@power.ufscar.br.

<sup>†</sup> Departamento de Química, Universidade Federal de São Carlos.

<sup>‡</sup> Departamento de Engenharia de Materiais, Universidade Federal de São Carlos.

<sup>§</sup> Universidade de São Paulo.

(1) Fisher, G. *Ceramic Bull.* **1986**, *65*, 1355.

(2) Shriver, D. F.; Farrington, G. C. *Chem. Eng. News* **1985**, *63*, 42.

(3) Duwez, P.; Odell, F.; Brown, F. H. *J. Am. Ceramic Soc.* **1952**, *35*, 107.

(4) Gupta, T. K.; Bechtold, J. H.; Kuznicki, R. C.; Cadoff, L. H.; Rossing, B. R. *J. Mater. Sci.* **1977**, *12*, 2421.

(5) Di Quarto, F.; Piazza, S.; Sunseri, C. *J. Electrochem. Soc.* **1984**, *131*, 2902.

(6) Leach, J. S. L.; Pearson, B. R. *Electrochim. Acta* **1984**, *29*, 1263.

(7) Leach, J. S. L.; Pearson, B. R. *Electrochim. Acta* **1984**, *29*, 1271.

(8) Khalil, N.; Bowen, A.; Leach, J. S. L. *Electrochim. Acta* **1988**, *33*, 1721.

(9) Patrino, E. M.; Torresi, R. M.; Leiva, E. P. M.; Macagno, V. A. *Electrochim. Acta* **1992**, *37*, 281.

(10) Patrino, E. M.; Macagno, V. A. *J. Electrochem. Soc.* **1993**, *140*, 1576.

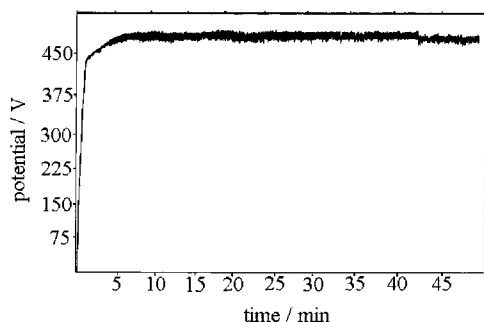


**Figure 1.** Chronopotentiogram obtained during the ZrO<sub>2</sub> film growth in 0.1 mol L<sup>-1</sup> H<sub>3</sub>PO<sub>4</sub> solution,  $i = 36 \text{ mA cm}^{-2}$ ,  $T = 5 \text{ }^\circ\text{C}$ .

solutions containing Na<sub>2</sub>[Ca(EDTA)] at different concentrations were investigated. The experiments were carried out at temperatures between 5 and 25 °C. Zirconium plates ( $A = 0.5 \text{ cm}^2$ ) and a semicircular platinum sheet ( $A = 21 \text{ cm}^2$ ) were used as working and auxiliary electrodes, respectively. The oxide growth was followed by potential–time curves. A power supply was used to generate the current between the working electrode and the auxiliary electrode.

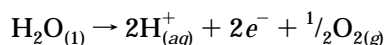
The crystalline structure of the oxide films was determined by XRD utilizing a Siemens D5000 diffractometer using a Cu anode (Cu K $\alpha = 1.5418 \text{ \AA}$ ). The morphology of the oxide films was characterized by a Zeiss 950 SEM and the presence of dopants on the oxide film was determined by energy-dispersive X-ray spectroscopy (EDX) using a PGT Prism spectrometer.

The surface analysis by XPS was performed using a Kratos XSAM HS spectrometer. The radiation source used to excite the photoelectrons was Mg K $\alpha$  energy of 1253.6 eV and power given by 15 kV and 15 mA. The pressure in the analysis chamber was  $10^{-9}$  Torr. The samples were flooded with low-energy electrons from a flood gun to avoid charging effects. The spectra were referenced to the carbon 1s line from adventitious hydrocarbons, set at 284.8 eV. Argon ion sputtering (3 kV, 20 mA) was employed to remove surface layers in order to analyze the variation of composition with depth.

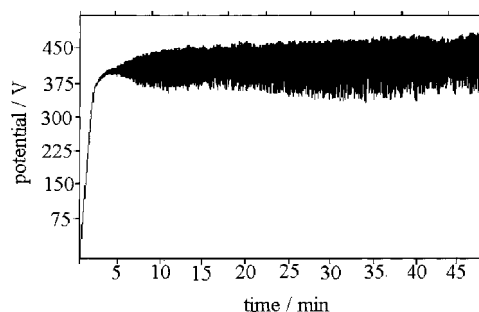
## Results and Discussion

Figure 1 shows a typical potential–time curve for the oxide film grown in phosphoric acid aqueous solutions. This curve is characterized by two regions: the initial region presents a linear increase of the potential, and in the second region almost no change in the average potential is observed, although it shows an oscillation of approximately 20 V. An electric field applied to an oxide film causes electric charge transport through the film. The charges can be carried by ions or electrons. Thus, in an experiment in which the charge flux, which is a linear function of the current density, is constant, there could be different processes contributing to this flux: ion transport,  $i_f$ , electronic transport,  $i_e$ , and dissolution current,  $i_d$ .

In the region of linear potential increase, the main contribution to the charge flux is the ionic conduction,  $i_f$ , which leads to an oxide film growth. On the other hand, the constant potential region is characterized by electronic conduction through the film from the solution interface due to the reaction:



In the intermediate region observed in Figure 1, the curve levels off, indicating that the values of  $i_d$  and  $i_e$  become important.



**Figure 2.** Chronopotentiogram for the ZrO<sub>2</sub> film growth in 0.1 mol L<sup>-1</sup> H<sub>3</sub>PO<sub>4</sub> solution with 0.1 mol L<sup>-1</sup> Na<sub>2</sub>[Ca(EDTA)] solution,  $i = 36 \text{ mA cm}^{-2}$ ,  $T = 5 \text{ }^\circ\text{C}$ .

The second region indicates that the oxide film suffers rupture by electronic<sup>11</sup> or mechanical processes.<sup>12</sup> The mechanical stress<sup>12</sup> can be generated inside the oxide film by interfacial tension of anion adsorption, electric field, hydration and dehydration processes, and the difference between metal molar volume and oxide molar volume due to the presence of impurities such as solution ions inside the film. Sato and Cohen<sup>12</sup> developed a model to describe the oxide film rupture by mechanical stress related to the electric field and interfacial tension. From another point of view, Ikonopisov<sup>11</sup> proposed the electron avalanche model. In this model,<sup>11</sup> the electrons resulting from the water oxidation reaction are accelerated by the electric field through the oxide film from the solution–oxide interface. The electron avalanche occurs due to defects in the oxide film like incorporated electrolyte anions. The electric field ionizes these defects and the electrons move from the impurity levels to the conduction band, accelerated by the field. The electrons collide with the oxide molecules and provoke new ionization, giving rise to the electron avalanche phenomenon. Sparks were observed in the oxide film surface after the beginning of the constant potential region.

For the film grown in phosphoric acid solution containing Na<sub>2</sub>[Ca(EDTA)] complex, presented in Figure 2, the potential curve as a function of time presents the same characteristics described in Figure 1 for the film grown in H<sub>3</sub>PO<sub>4</sub> solution, although the potential breakdown occurs at lower values, indicating the presence of defects in the oxide film. The increase of the potential oscillations with time in Figure 2 probably is related to the increase of the defect density in the oxide.

The morphology of the oxide films prepared in pure H<sub>3</sub>PO<sub>4</sub> is completely different than the morphology of the oxide films grown in the presence of Na<sub>2</sub>[Ca(EDTA)] complex. The oxide films prepared in 0.1 mol L<sup>-1</sup> H<sub>3</sub>PO<sub>4</sub> solution showed a compact and uniform microstructure, while the ones prepared in the presence of calcium complex were porous, as shown in parts a and b of Figure 3, respectively. We performed qualitative EDX microanalysis in the film shown in Figure 3 and detected Zr, Ca, and O.

We employed XPS to characterize the oxide film surfaces in order to identify the chemical states and determine the amounts of the elements. The Zr 3d spectra are shown in parts a and b of Figure 4 for the ZrO<sub>2</sub> films prepared in aqueous H<sub>3</sub>PO<sub>4</sub> and in the

(11) Ikonopisov, S. *Electrochim. Acta* **1977**, *22*, 1077.

(12) Sato, N.; Cohen, M. *J. Electrochem. Soc.* **1964**, *111*, 512.

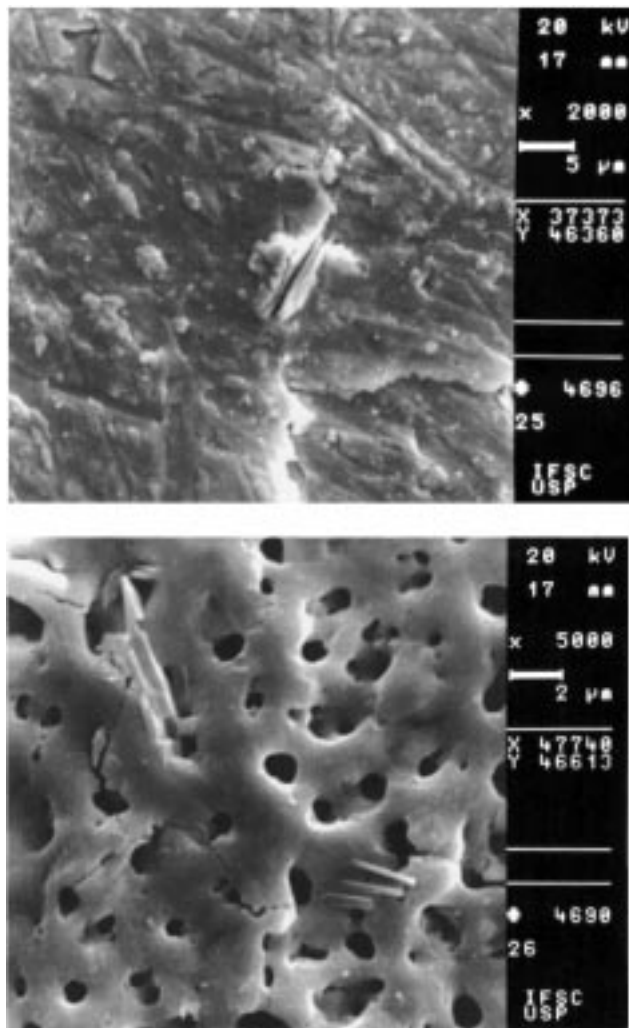


**Figure 3.** (a) Micrograph of the  $\text{ZrO}_2$  film growth in  $0.1 \text{ mol L}^{-1} \text{H}_3\text{PO}_4$  solution and (b)  $\text{ZrO}_2$  film growth in  $0.1 \text{ mol L}^{-1} \text{H}_3\text{PO}_4$  solution with  $0.1 \text{ mol L}^{-1} \text{Na}_2[\text{Ca}(\text{EDTA})]$ ,  $i = 5 \text{ mA cm}^{-2}$ ,  $T = 20 \text{ }^\circ\text{C}$ .

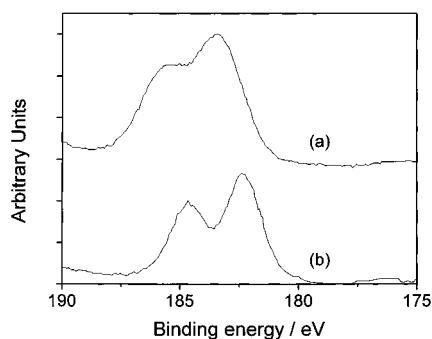


**Figure 4.** (a) Zr 3d XPS results for the  $\text{ZrO}_2$  films prepared in aqueous  $0.1 \text{ mol L}^{-1} \text{H}_3\text{PO}_4$  and (b) Zr 3d XPS results for the  $\text{ZrO}_2$  film growth in  $0.1 \text{ mol L}^{-1} \text{H}_3\text{PO}_4$  solution with  $0.1 \text{ mol L}^{-1} \text{Na}_2[\text{Ca}(\text{EDTA})]$ ,  $i = 5 \text{ mA cm}^{-2}$ ,  $T = 20 \text{ }^\circ\text{C}$ .

presence of  $0.1 \text{ mol L}^{-1}$  calcium complex, respectively. The shapes of the Zr 3d photoelectron doublets differ, as well as their binding energies, indicating that the calcium oxide-doped film, with a binding energy of 182.3 eV, is consistent with  $\text{ZrO}_2$ , while the film grown in the  $\text{H}_3\text{PO}_4$  solution, with a binding energy of 183.3 eV, could be related to the formation of a Zr-OH species.<sup>13</sup>

The XRD spectrum shows that the oxide films grown from aqueous phosphoric acid solutions without the Ca

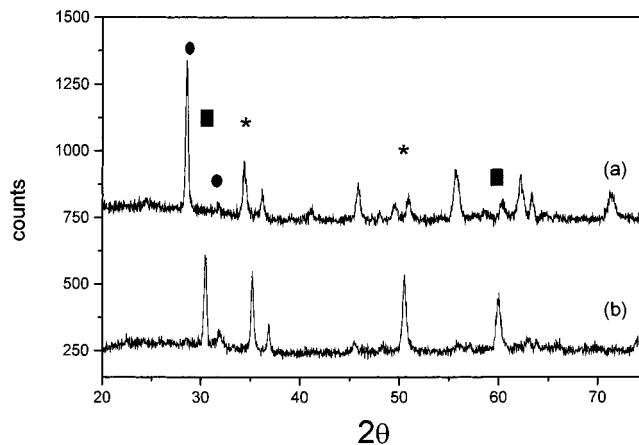


**Figure 5.** X-ray diffraction spectrum for (a)  $\text{ZrO}_2$  film growth in aqueous  $0.1 \text{ mol L}^{-1} \text{H}_3\text{PO}_4$  solution (b) for  $\text{ZrO}_2$  film growth in aqueous  $0.1 \text{ mol L}^{-1} \text{H}_3\text{PO}_4$  solution with  $0.1 \text{ mol L}^{-1} \text{Na}_2[\text{Ca}(\text{EDTA})]$ ,  $i = 36 \text{ mA cm}^{-2}$ ,  $T = 5 \text{ }^\circ\text{C}$ . (●) peaks associated with the baddeleyite phase of zirconium oxide; (■) peaks associated with the cubic phase of zirconium oxide; (\*) peaks associated with metallic zirconium.

complex are crystalline and have monoclinic structure, as can be observed in Figure 5a. The oxide film prepared in aqueous phosphoric acid solutions in the presence of the Ca complex presents a completely different XRD diffraction pattern (Figure 5b). In Figure 5b, the presence of the peaks which characterize the cubic structure of zirconium oxide is observed for this latter case.

The conventional method of zirconium oxide stabilization is based on mixing oxide phases followed by sintering at high temperatures. A possible explanation for our results is that the grain sizes in the film are small enough to predominantly lead to the crystallization of zirconium oxide in the tetragonal phase at low temperatures, according to Gravie's model.<sup>14</sup> This model<sup>14</sup> also states that when the grains grow as the sample is thermally treated, zirconium oxide is converted to monoclinic phase. To investigate this possibility, the metal substrate was treated at  $800 \text{ }^\circ\text{C}$  in order to grow a thermal oxide. Then, the metal was anodized in aqueous solution of  $0.1 \text{ mol L}^{-1} \text{H}_3\text{PO}_4$  with  $0.1 \text{ mol L}^{-1}$  Ca complex. This oxide was peeled off from the electrode and then treated at  $1100 \text{ }^\circ\text{C}$ . It was necessary to scrape off the oxide film from the substrate to avoid further oxide growth on the metal. The results for the original oxide film thermally formed at  $800 \text{ }^\circ\text{C}$ , the anodically prepared oxide film treated at  $800 \text{ }^\circ\text{C}$ , and the powder oxide peeled off from the electrode and treated at  $1100 \text{ }^\circ\text{C}$  are shown in Figure 6. It can be observed that the thermally formed film presents a monoclinic phase. After the anodization, the oxide is partially converted to the cubic phase. The powder, after thermal treatment at  $1100 \text{ }^\circ\text{C}$ , presents more cubic phase than the oxide treated at  $800 \text{ }^\circ\text{C}$ . This could be related to the accumulation of CaO in the surface and later diffusion through the oxide during the high-temperature treatment. Therefore, the proposition that the  $\text{ZrO}_2$  prepared by the electrochemical method is stabilized in the cubic phase by a size effect<sup>14</sup> can be excluded.

The aforementioned mechanism is not the only one

(13) Li, Y. S.; Wong, P. C.; Mitchell, K. A. R. *Appl. Surf. Sci.* **1995**, *89*, 263.

(14) Gravie, R. C. *J. Phys. Chem.* **1978**, *82*, 218.

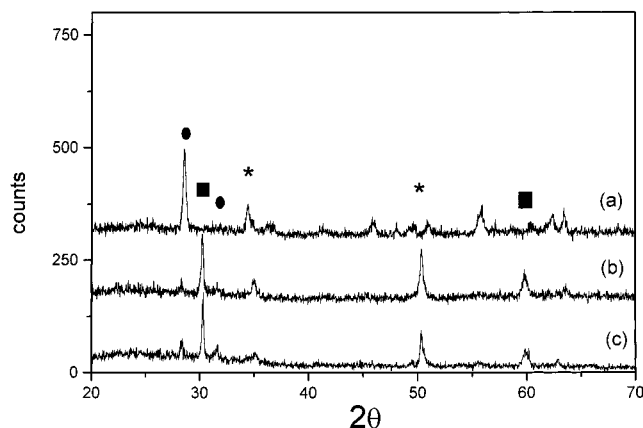


**Figure 6.** X-ray diffraction patterns for  $\text{ZrO}_2$  films: (a) thermal oxide prepared at 800 °C for 2 h, (b) oxide film prepared anodically after substrate treatment at 800 °C, and (c) powder from the film described for part b after treatment at 1100 °C. Anodically grown in aqueous 0.1 mol  $\text{L}^{-1}$   $\text{H}_3\text{PO}_4$  solution with 0.1 mol  $\text{L}^{-1}$   $\text{Na}_2[\text{Ca}(\text{EDTA})]$ .  $i = 36 \text{ mAcm}^{-2}$ .  $T = 5 \text{ °C}$ . (●) peaks associated with the baddeleyite phase of zirconium oxide; (■) peaks associated with the cubic phase of zirconium oxide; (\*) peaks associated with metallic zirconium.

that could explain our results. Another possibility for the zirconium oxide stabilization by the electrochemical method is associated with the breakdown phenomenon of the oxide film. In agreement with the Ikonopisov model,<sup>11</sup> the applied electric field can ionize and accelerate the defects present on the oxide film. The resulting electrons collide with the oxide molecules, causing new ionization processes, initiating the electron avalanche phenomenon schematically presented in Figure 7, which locally leads to the film's destruction. As a consequence, the electrolytic solution penetrates into the oxide film carrying away the ions present in this phase. Corroborating with this statement, results of the quantification of these ions obtained by the combination of XPS and argon ion sputtering presented in Table 1 indicate that the concentration of calcium is higher in the film surface (accordingly to longer sputtering times). Simultaneously, the applied current is concentrated at this point because the local electrical resistance is much lower than the oxide resistance, since the film is thinner at the pore. The conduction of a high current around a porous channel as thin as 1  $\mu\text{m}$  generates heat dissipation high enough to promote the decomposition and vaporization of the electrolyte inside the holes, forming the doped zirconium oxide (Figure 7). Semiquantitative EDX measurements showed that the bulk concentration of calcium in the oxide was approximately 12 atom %. The  $\text{Ca}/\text{Zr}$  ratio calculated from Table 1 decreases with sputtering time, indicating that the concentration of calcium ions in the film is higher at the surface than in the bulk. The other ions detected by XPS, Na and P, arise from the solution and remain on the film surface after the solution vaporization process.

### Conclusions

In this paper we described a new method to introduce large quantities of dopants in oxide films and demon-

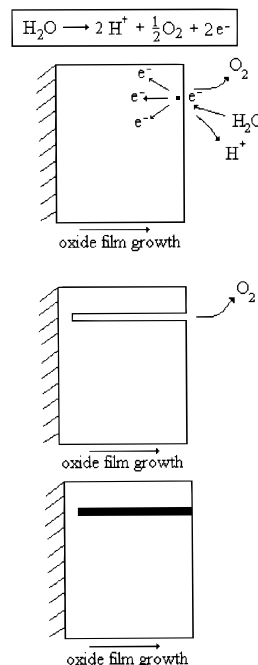


**Figure 7.** Schematic representation of the breakdown phenomena which leads to the zirconium oxide stabilization in the cubic phase.

**Table 1. Quantification (atom %) Measured by XPS for Different Ion Sputtering Times for the  $\text{ZrO}_2$  Film Grown in Phosphoric Acid Solution Containing  $\text{Na}_2[\text{Ca}(\text{EDTA})]$  Complex**

element	quantification (atomic %) for different ion sputtering times			
	no ion sputtering	60 min	120 min	240 min
O	47.3	41.5	38.1	39.1
C	40.7	41.2	38.4	36.5
N	2.0	3.0	5.3	2.3
Na	0.8	1.8	1.1	1.0
P	3.2	3.9	8.3	5.4
Ca	4.5	6.2	6.2	10.2
Zr	1.5	2.5	2.5	5.5

strated the viability of preparing stabilized zirconium oxide films at room temperature using electrochemical methods. The film grown in the presence of  $\text{Na}_2[\text{Ca}(\text{EDTA})]$  complex was cubic, as indicated by XRD, SEM, and XPS measurements. The electrochemical oxide growth was characterized by an initial linear potential increase, which was related only to the oxide growth. A second region, with an oscillatory potential behavior, was related to the breakdown phenomenon. We proposed that the local destruction and rebuilding of the oxide film lead to the incorporation of the solution ions. These ions migrate into the oxide during the film rebuilding as the electric current flows through the pores created by the local film destruction.

**Acknowledgment.** The authors would like to thank H. A. Carmona for his assistance in some of the XPS measurements. This work was supported by CNPq, FAPESP, and PADCT II of Brazil.

CM980508P